INTERNATIONAL JOURNAL OF HYDROGEN ENERGY 43 (2018) 23221–23230

Available online at www.sciencedirect.com

ScienceDirect

journal homepage: www.elsevier.com/locate/he

High performance electrocatalysts supported on graphene based hybrids for polymer electrolyte membrane fuel cells

Begüm Yarar Kaplan [a], Navid Haghmoradi [b], Emre Biçer [a], César Merino [c], Selmiye Alkan Gürsel [a,b,*]

[a] Sabanci University Nanotechnology Research & Application Center (SUNUM), Sabanci University, Istanbul, 34956, Turkey

[b] Faculty of Engineering and Natural Sciences, Sabanci University, Istanbul, 34956, Turkey

[c] Grupo Antolin Ingeniería, Burgos, E09007, Spain

ARTICLE INFO

Article history:
Received 1 April 2018
Received in revised form
16 July 2018
Accepted 29 October 2018
Available online 22 November 2018

Keywords:
Graphene
Hybrid catalyst support
Pt nanoparticle
Electrocatalyst
PEM fuel cell

ABSTRACT

In this study, new electrocatalysts for PEM fuel cells, based on Pt nanoparticles supported on hybrid carbon support networks comprising reduced graphene oxide (rGO) and carbon black (CB) at varying ratios, were designed and prepared by means of a rapid and efficient microwave-assisted synthesis method. Resultant catalysts were characterized *ex-situ* for their structure, morphology, electrocatalytic activity. In addition, membrane-electrode assemblies (MEAs) fabricated using resultant electrocatalysts and evaluated *in-situ* for their fuel cell performance and impedance characteristics. TEM studies showed that Pt nanoparticles were homogeneously decorated on rGO and rGO-CB hybrids while they had bigger size and partially agglomerated distribution on CB. The electrocatalyst, supported on GO-CB hybrid containing 75% GO (HE75), possessed very encouraging results in terms of Pt particle size and dispersion, catalytic activity towards HOR and ORR, and fuel cell performance. The maximum power density of 1090 mW cm^{-2} was achieved with MEA (Pt loading of 0.4 mg cm^{-2}) based on electrocatalyst, HE75. Therefore, the resultant hybrid demonstrated higher Pt utilization with enhanced FC performance output. Our results, revealing excellent attributes of hybrid supported electrocatalysts, can be ascribed to the role of CB preventing rGO sheets from restacking, effectively modifying the array of graphene and providing more available active catalyst sites in the electrocatalyst material.

Introduction

The need for more sustainable energy resources and the environmental issues regarding fossil fuels lead to serious challenges in protecting the environment and energy policy around the world. One promising solution is the fuel cell technology, which provides a clean and sustainable electricity source. Fuel cells directly convert the chemical energy of oxygen and fuel to electricity by electrochemically reducing the

* *Corresponding author*. Sabanci University Nanotechnology Research & Application Center (SUNUM), Sabanci University, Istanbul, 34956, Turkey.
E-mail address: selmiye@sabanciuniv.edu (S. Alkan Gürsel).

https://doi.org/10.1016/j.ijhydene.2018.10.222

oxygen and oxidizing fuel to produce water and release heat as the only by-products. PEM (polymer electrolyte membrane) fuel cells have demonstrated high energy efficiency and power density [1–3]. A crucial issue of PEM fuel cell development in large-scale application is reducing the platinum (Pt) loading because of its cost and supply limitation [4]. This issue can be overcome by designing catalysts with high electrocatalytic activity [5,6]. Most of the studies about catalyst materials exhibiting high electrocatalytic activity have focused on catalyst and catalyst support with high surface area [7–9].

The catalyst nanoparticles are needed to be dispersed on a conductive support which is usually a carbon-based material [10–14]. It is generally accepted that carbon support promotes the catalyst materials dispersion, electron transportation, and the kinetics of mass transfer at the electrode surface [15]. Furthermore, the utilization of nanostructured carbonaceous materials as the catalyst support presents a promising option for the catalysts with high electrocatalytic activity for fuel cells [16]. In addition, for the further enhancement of the electrocatalytic activity and stability it is necessary to increase the interaction between Pt and its supports, in order to inhibit the tendency of Pt nanoparticle coalescence [11].

The most extensively utilized catalyst support is carbon black (CB) for PEM fuel cell [17]. However, carbon black suffers from corrosion under high voltage conditions which results in Pt agglomeration and then dissolution into membrane [18–20]. To overcome that significant problem, alternative carbon materials [21–24], carbon based hybrids [2,25,26] and composites [27–29] were employed as catalyst supports for PEM fuel cells.

Recently, graphene owing to its two dimensional structure has been employed as an alternative catalyst support for PEM fuel cell [30–34]. Although graphene provides better Pt dispersion on the surface, and excellent electrical conductivity, restacking of individual graphene sheets cause a decrease in active sites and Pt utilization on the carbon support [35–37]. There are many strategies to improve Pt utilization and active sites of graphene. One strategy is to add more ionomer to the catalyst layer, thereby increasing the interface between Pt nanoparticles (NPs) and the ionomer [38]. Although that approach is acceptable, surplus ionomer causes additional issues including formation of thicker ionomer film onto the catalyst surface, decreasing the electronic conductivity and limited diffusion (mass transport) of reactant gases in the catalyst layer [39]. To overcome this problem, many researchers have tried to integrate carbon based nanostructured materials between graphene sheets. Different carbon-based materials such as carbon black [11,36,39,40], carbon nanotube [41,42], and carbon fiber [43] have been employed for this reason. Yet, by this way, preferred horizontal stacks of graphene are dislocated causing the formation of randomly distributed sheets in the catalyst layer (CL) [16]. CB is one of the most promising candidate that can help avoiding restacking of graphene sheets owing to its low price and high electronic conductivity [39]. Li et al. [11] studied the preparation of hybrid Pt/rGO-CB by mixing Pt/rGO with CB. Pt/rGO-CB's considerably higher ORR activity with respect to simple Pt/rGO catalyst has been reported. However, fuel cell performance was not reported in their study. In another relevant study, Cho et al. [36] showed that Pt/GN (graphene single nanosheet) electrocatalyst when intercalated with CB provided higher electrocatalytic activity for hydrogen oxidation, and enhanced performance in PEM fuel cell, especially in the activation and mass transport losses region of polarization curve, were observed. In all these studies, CB were used as a spacer, but it is not supporting Pt nanoparticles (NPs) on the surface. Here the other problem is that although non-reactive CB could increase conductivity, resultant catalyst layer would be so thick that increase mass transfer resistance, block Pt active sites and incline the corrosion. Therefore, on one hand, CB in hybrid catalyst structure directly influences the fuel cell performance. On the other hand, CB content is critical and should be meticulously optimized. Previously, it was shown that amount of CB should be minimized to provide better Pt activity and fuel cell performance [26,36,40].

Supported Pt NPs are synthesized by various methods [31–33,44]. $NaBH_4$ [45,46], L-ascorbic acid [47], citric acid [48] or ethylene glycol [49,50] were used as the reducing agents in the case of chemical reduction methods. When ethylene glycol is employed, metal NPs with smaller size and good dispersion on catalyst support can be obtained; however, due to weak reduction ability of ethylene glycol higher reaction temperature (>120 °C) and longer time (>4 h) [49] are required. Microwave (MW) irradiation is an alternative method which is usually more suitable, than conventional chemical synthesis/reduction by heating, owing to its simplicity, fast procedure, and the product's uniformity [51,52]. Moreover, MW method yields smaller and well dispersed Pt NPs compared to conventional heating method. Moreover, Pt NPs particle size can be well controlled by adjustment of pH [53].

In this study, Pt NPs supported on GO-CB hybrids as the electrocatalysts for fuel cell reactions were synthesized using one-pot microwave-assisted reduction method. For that purpose, GO and CB mechanically mixed in varying ratios first unlike previous studies and subsequent deposition of Pt NPs on hybrid support and simultaneous reduction of GO to rGO in hybrid were performed. In this facile process, the usage of CB prevents restacking of graphene sheets, and also Pt NPs were impregnated on both graphene and CB. The homogenous mixing of GO and CB resulted in formation of 3D CB entangled between the 2D graphene sheets (Fig. 1). Resultant electrocatalysts were characterized both *ex-situ* for their structure, morphology, electrocatalytic activity, and *in-situ* for their fuel cell performance and impedance characteristics. Compared to previous studies in literature [2,11,39], we have investigated electrochemical characteristics of hybrid electrocatalysts, comprising graphene oxide (GO) and carbon black at varying ratios, by *ex-situ* and *in-situ* techniques in detail.

Experimental

Materials

Graphene oxide (GO) was supplied from Grupo Antolin Ingenieria SA. Vulcan XC-72 (commercial CB) was purchased from Fuel Cell Earth LCC and Nafion® solution (20 wt% alcohol based), chloroplatinic acid (H_2PtCl_6), dimethylformamide (DMF) (C_3H_7NO), ethylene glycol, 2-propanol were purchased from Sigma-Aldrich. Sigracet 39BC GDL (FuelCellStore),

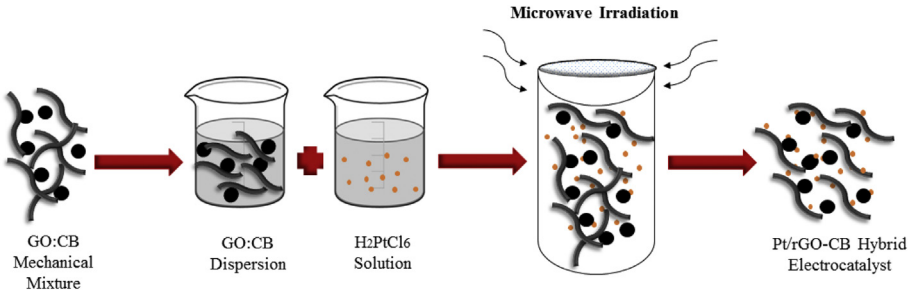

Fig. 1 – Schematic of microwave assisted synthesis of Pt/rGO-CB.

Nafion® NR212 membrane (FuelCellStore), 30% Pt on Vulcan XC-72, Nafion® solution and 2-propanol were used for electrode preparation.

Synthesis of electrocatalysts by microwave-assisted reduction method

Pt NPs were deposited on carbon supports (CB, GO and GO-CB hybrids) by microwave-assisted reduction method. In these electrocatalysts, varied weight to weight ratios of GO to CB, were employed during the synthesis as depicted in Table 1. In a typical synthesis, 100 mg of the carbon support was dispersed in 4:1 (v:v) ethylene glycol:2-propanol and sonicated until complete dispersion. 1.5 times of H_2PtCl_6 was added to 4 mL of ethylene glycol solution with respect to catalyst support and stirred for 2 h. This solution was then added to the dispersed catalyst support solution and mixed until complete dispersion. The pH of the solution was adjusted to 12 with 1 M NaOH (in ethylene glycol). The mixture was then irradiated in a microwave reactor (Anton-Paar Microwave Synthesis Reactor Monowave 300) at 500 W/65 s followed by cooling at room temperature. To control Pt NPs size, the pH of the above mentioned irradiated solution was adjusted to 4 by dropwise addition of 0.5 M HNO_3. The obtained Pt/CB, Pt/rGO and Pt/rGO-CB were washed and filtered with DI water six times and dried in oven at 60 °C for 24 h. All Pt/CB, Pt/rGO, and Pt/rGO-CB hybrid electrocatalysts were synthesized.

Ex-situ characterization of electrocatalysts

XRD analyses of carbon supports and crystalline diffraction patterns of electrocatalysts were carried out by using Bruker D-8 Advance X-Ray Diffractometer (wavelength of irradiation of Cu Kα of 0.154 nm, at 2θ angles 5° –90°, scan rate of 2.4° per minute with the operating voltage of 40 kV and current of 40 mA). Graphitic structure of carbon supports and investigation of NPs were obtained with Renishaw in Via Raman Spectrometer with a laser excitation line of 532 nm. TEM (FEI-Tecnai G2 F30) was employed for the determination of Pt particle size and distribution. The sample preparation for TEM involved the dispersion of the suspension in IPA and collected onto a holey carbon coated TEM grid. Particle size of electrocatalysts were determined from HR-TEM images by using Image J software. X-ray Photoelectron Spectroscopy (XPS) was used to analyze chemical structure of electrocatalysts and Pt NPs reduction on support recorded by using a high-resolution Thermo Specific X-ray Photoelectron Spectrometer with monochromatic Al Kα X-ray source.

Table 1 – Electrocatalysts prepared at varying rGO to CB weight ratios (HE stands for hybrid electrocatalysts).

Electrocatalyst	GO:CB (w:w)
HE00 (Pt/CB)	0:100
HE25 (Pt/rGO-CB)	25:75
HE50 (Pt/rGO-CB)	50:50
HE75 (Pt/rGO-CB)	75:25
HE100 (Pt/rGO)	100:0

Electrochemical characterizations

3-electrode system was employed to determine electrochemical characteristics of electrocatalysts. In this system, glassy carbon rotating disk electrode (RDE) as the working (WE), Pt wire as the counter (CE), and Ag/AgCl as the reference electrode (RE) were employed. 2 mg of catalyst as powder was dispersed in 1 mL of DMF, 2-propanol (1:4 in volume) mixture/Nafion® solution (20%) (50:1 w/w) and ultrasonicated for 2 h to acquire the homogeneous catalyst ink. Then, catalyst ink was applied dropwise onto polished glassy carbon electrode. The Pt loading of each catalyst was kept constant as 20 μg_{Pt} cm^{-2}. The electrolyte (0.1 M $HClO_4$) was purged with N_2 for 30 min for CV, and O_2 purged for 30 min for LSV experiment. WE was activated and stabilized by 50 cycles at a scan rate of 100 mV s^{-1}. HOR CV curves were obtained in N_2-saturated 0.1 M $HClO_4$ without rotation between −0.2 and 1.2 V, at a scan rate of 50 mV s^{-1}. LSV measurements for ORR were performed in O_2-saturated 0.1 M $HClO_4$ between 0.0 and 1.0 V at a scan rate of 10 mV s^{-1} and rotation speed of 1600 rpm. In the CV and LSV experiments, the measured potentials vs. the reference were converted to RHE scale with using the Nernst equation;

$$E_{RHE} = E_{Ag/AgCl} + 0.059pH + E^0_{Ag/AgCl}$$

where E_{RHE} is the converted electrode potential vs. RHE, $E_{Ag/AgCl}$ is the measured potential vs. Ag/AgCl RE, and $E^0{}_{Ag/AgCl}$ is the standard electrode potential of Ag/AgCl at 25 °C which is 0.1976 V.

Fuel cell testing

For the fabrication of cathode, catalyst ink was prepared by sonicating prepared electrocatalysts (Pt/CB, Pt/rGO, or Pt/rGO-CB hybrids; 30 wt% Pt on support), Nafion® solution (20 wt%) and 2-propanol, stirring them for 2 h. For anode, catalyst ink

was a dispersion of commercial Pt/CB catalyst powder (30 wt% Pt on carbon black), and Nafion® solution (20 wt%) in IPA. The catalyst ink was exerted on the gas diffusion layer by spraying method to form gas diffusion electrode (GDE). After drying GDE at 60 °C for 10 min, the spraying procedure was repeated multiple times until 0.4 mg_{Pt} cm^{-2} loading was achieved. Sprayed GDEs (anode and cathode with 5 cm^2 area) were hot pressed at 133 °C onto Nafion® NR212 membranes 133 °C and 2 MPa for 5 min after 10 min pre-heating step at 133 °C without applying pressure. The fuel cell tests were performed in a fully humidified atmosphere at 80 °C with 500 cc/min of H_2 and O_2 with using 850e fuel cell test station (Scribner Associates, USA).

The MEAs were also characterized by in-situ by electrochemical impedance spectroscopy (EIS). The AC impedance arcs were recorded by sweeping frequencies over a frequency range of 10 kHz–0.1 Hz at an amplitude of 10% of DC at the potential of 0.70 V (80 °C, fully humidified H_2/O_2, 1 $atm_{absolute}$ conditions).

Results and discussion

The XRD spectra of Pt/rGO-CB hybrid, Pt/CB, and Pt/rGO electrocatalysts are shown in Fig. 2. All electrocatalysts exhibited representative diffraction peaks at 39.8°, 46.5°, 68.7°, and 82.1° which correspond to the (111), (200), (220), and (311) planes of the FCC structure of Pt [53]. This shows the successful Pt decoration on CB, rGO, and rGO-CB hybrid supports. Moreover, the peak at 26.2° is associated with C(002) diffraction peak of graphitic structure of carbon materials, and prove more crystalline, a sp^2 carbon network was regenerated [15,54]. This peak was formed via the movement of characteristic broader peak of GO at around 12° at the end of reduction process [55].

Fig. 3 demonstrates the Raman spectra of GO, Pt/rGO (HE100) and Pt/CB-rGO (HE75). The two distinguished characteristic peaks at 1340 and 1590 cm^{-1} correspond to the D band which is generated due to sp^2 hybridized graphitic carbon

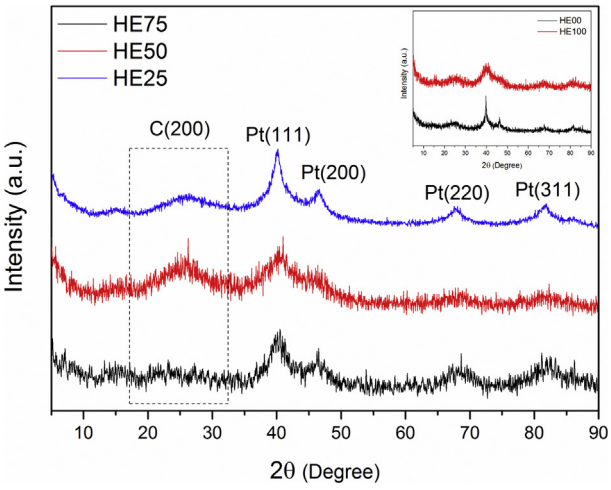

Fig. 2 – XRD spectra of Pt/rGO-CB hybrids, Pt/CB, and Pt/rGO electrocatalysts (Inset: XRD spectra of pristine GO and CB).

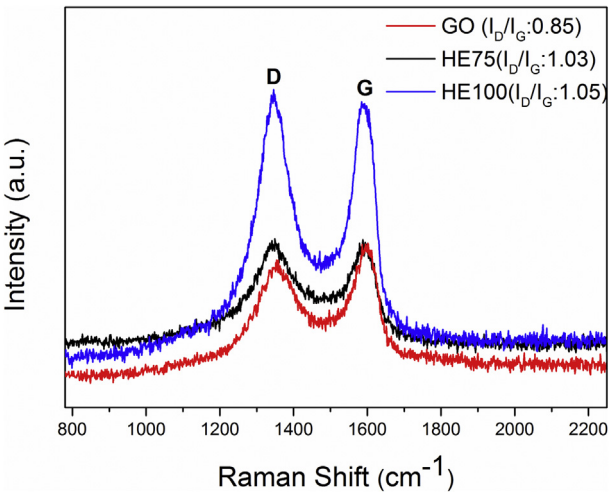

Fig. 3 – Raman spectra of GO, Pt/rGO (HE100), and Pt/rGO-CB (HE75).

atoms, and the G band which is generated due to sp^3 hybridized carbon atoms of disordered graphene [56]. The intensities of G and D peaks and the comparison of them provide a significant information about structural organization of atoms. Using the I_D/I_G ratio of GO (0.85) as a reference, the I_D/I_G ratios increased to 1.05 for Pt/rGO (HE100), and 1.03 for Pt/rGO-CB (HE75), respectively. The increased I_D/I_G indicates the enhanced defects in graphene structure as a result of electronic interaction with metal NPs [57], and confirms the formation of rGO [58].

Chemical structure of surface of the electrocatalysts were investigated further by XPS. In order to analyze the oxidation state of Pt metal on CB, rGO, and rGO-CB hybrid high-resolution XPS analyses were performed on Pt/CB, Pt/rGO, Pt/rGO-CB electrocatalysts and the recorded spectra were depicted in Fig. 4(a, c, and e). The C 1s XPS peak of carbon supports are deconvoluted into four peaks of C=C, C-OH, O-C-O, and C=O/O-C=O corresponding to the binding energy of around 284.6, 286.0, 284.07, 287.6, and 288.8 eV, which coincides with oxidized functional groups including hydroxides (C-OH), epoxy-ether (C-O-C) and carbonyl-ketone, and carboxyl (C=O/O-C=O) in the carbon structure [59]. Functional groups intensities are very low due to removal of surface groups simultaneously with impregnation-reduction of Pt especially on the GO surface [49,60].

The Pt 4f XPS spectra of the electrocatalysts (Fig. 4b,d, and e) showed doublet peaks at 71.8 eV and 75.2 eV. The doublet peaks can be de-convoluted into three types of peaks at around 71.5 eV and 75.0 eV, 72.8 eV and 76.3 eV, and 74 eV and 77.5 eV that can be ascribed to Pt^0, Pt^{2+}, and Pt^{4+} states, respectively. It is clearly observed that the intensities of peaks, which correspond to Pt^{+2} and Pt^{+4} states, are very low. Moreover, two asymmetric-shaped signals are clearly observable at binding energies at around 71.8 and 75.2 eV with a well-separated spin-orbit components that are readily assignable to $4f_{7/2}$ and $4f_{5/2}$ core-levels of metallic Pt [61]. The presence of Pt^{2+} and Pt^{4+} species in the reduction of H_2PtCl_6 result from the two-step reduction process in which Pt (IV) reduces to Pt (II) and then reaches to its metallic form [62].

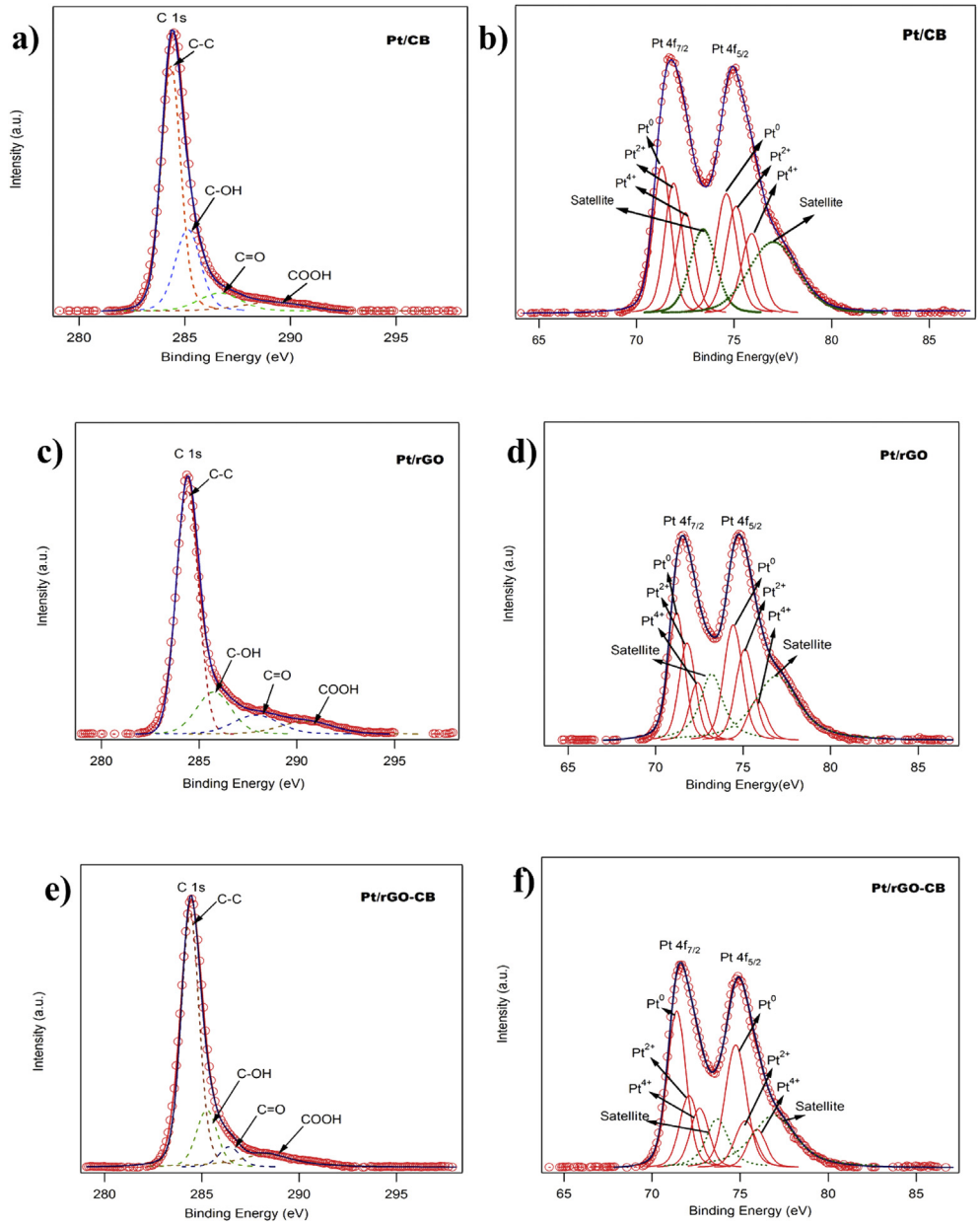

Fig. 4 – De-convoluted XPS spectrums a) C1s for Pt/CB, b) Pt 4f for Pt/CB, c) C1s for Pt/rGO, d) Pt 4f for Pt/rGO, e) C1s for Pt/rGO-CB (HE75), f) Pt 4f for Pt/rGO-CB (HE75).

The distribution and particle size of Pt on various carbon supports were investigated by TEM. As clearly seen from Fig. 5, Pt NPs were successfully deposited on all the carbon-based supports with a mean diameter 1.5–2.0 nm. Fig. 5c maintains a perfectly distributed Pt NPs on top of thin layer of graphene sheets having a mean diameter of Pt NPs 1.3 nm. Moreover, TEM image of Pt nanoparticles on CB (Fig. 5a) represented larger particle diameters (2.0 nm) with some partial agglomerations. TEM images provide the evidence that rGO might be better candidate than CB by having a larger surface area for Pt nanoparticle impregnation and homogeneous distribution. Since comparably larger Pt NPs were obtained during impregnation on CB, CB amount in hybrid content was very essential and had to be optimized. It can be inferred from Fig. 5, Pt NPs homogeneously distributed all over the hybrid support surface with larger particle size than Pt/rGO and smaller than Pt/CB. In order to obtain superior catalytic activity from Pt NPs, it is therefore essential that CB content should be minimized.

CV was performed to determine the electrochemical surface area (ECSA) of electrocatalysts which can provide a valuable data about the amount of active sites and electrocatalytic activity for HOR [63]. As depicted in Fig. 6a, all electrocatalysts have two distinct characteristic peaks, corresponding to the hydrogen adsorption or desorption regions below 0.4 V and the Pt oxidation or reduction regions in the range of 0.6–1.2 V without a noticeable change in the curve shape. Pt/rGO showed a comparable ECSA (54.8 m^2g^{-1}) with Pt/CB (50.0 m^2g^{-1}). Moreover, HE75 electrocatalyst exhibited highest ECSA (65.1 m^2g^{-1}) (Fig. 6b and Table 2) and

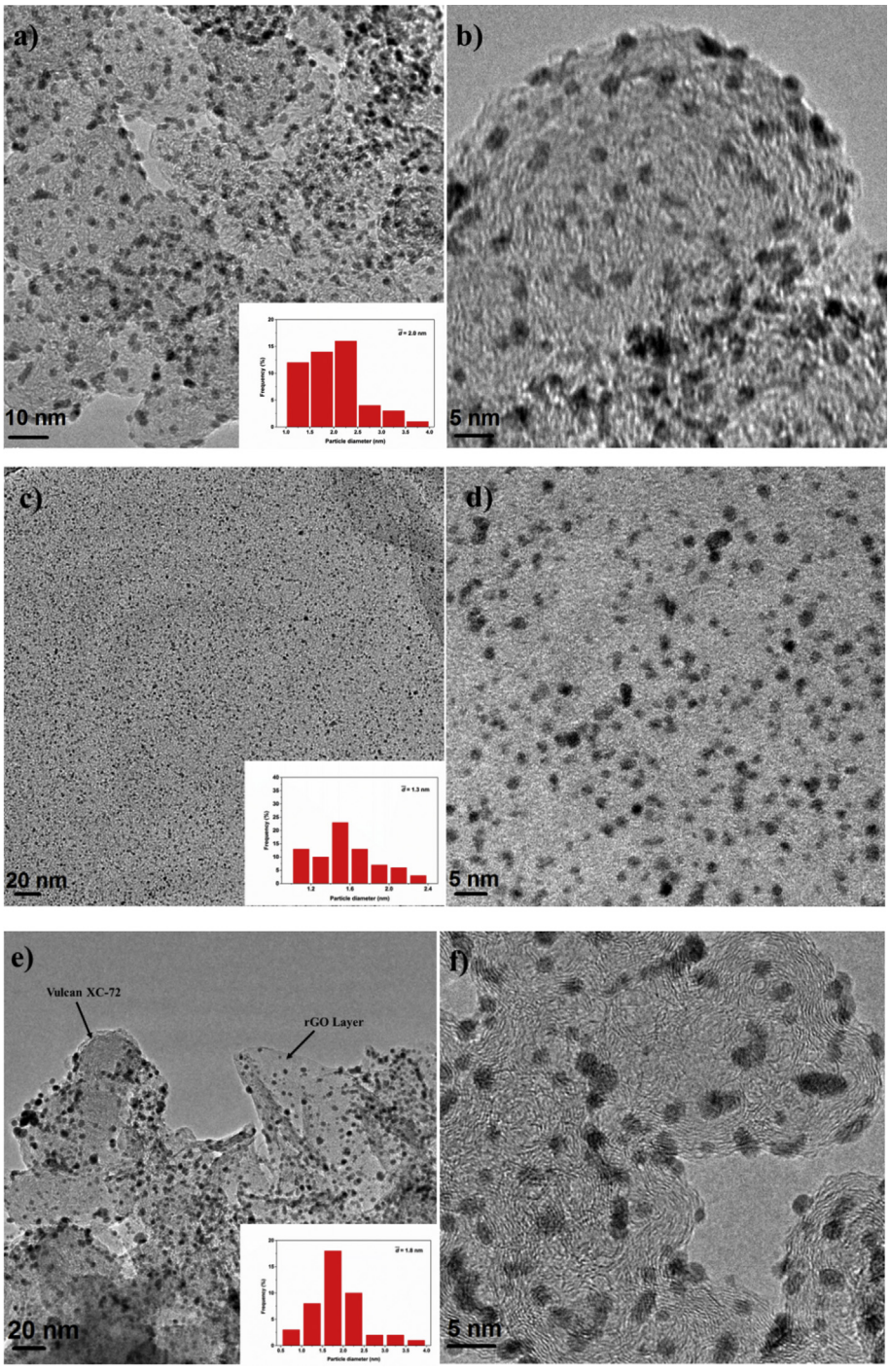

Fig. 5 – TEM micrographs of a) and b) HE00; c) and d) HE100; e) and f) HE75 (insets, Pt particle size distribution histograms).

therefore, superior electrocatalytic activity. It can be described by hybrid support network and improved electrical conductivity which promoted to fast electron transfer of support. In addition, better utilization of Pt NPs is expected because of rGO and CB's synergy. Furthermore, initial physical mixing of CB and rGO before the Pt assembly provides better Pt dispersion by limiting graphene restacking. Compared to hybrids obtained with addition of CB to the Pt/rGO electrocatalyst in literature, enhanced electrochemical activity and ECSA was obtained for Pt/rGO-CB (HE75) hybrid [64].

To examine the ORR of the synthesized Pt/rGO-CB hybrid electrocatalysts, the RDE measurements at 1600 rpm was carried out, as given in Fig. 6c. From the LSV curve, the diffusion-limiting currents for ORR on five electrocatalysts were realized to below 0.7 V. On the contrary, a mixed kinetic-diffusion controlled region appears from 0.7 V to 0.85 V. Therefore, related mass activity calculation results were given at 0.8 V. Superior activity of Pt/rGO-CB (HE75) hybrid electrocatalyst was demonstrated in terms of both half-wave potential and mass activity (Table 2). Clearly, a significant

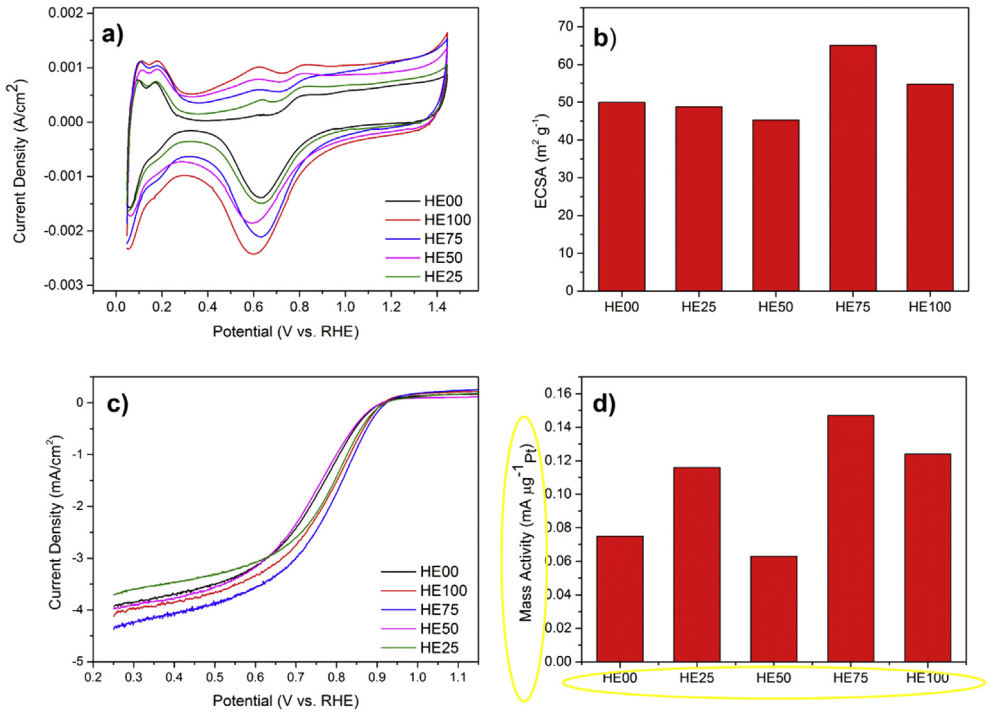

Fig. 6 – a) CV curves for HOR, b) Comparison of ECSA values, c) LSV curves for ORR and d) ORR mass activities of electrocatalysts.

Table 2 – ECSA, $\Delta E_{1/2}$, mass Activity, power output values of the Pt/rGO-CB electrocatalysts with varying composition.

Catalysts	ECSA (m^2g^{-1})	$\Delta E_{1/2}$ (V)	Mass Activity at 0.80 V (mA μg^{-1} $_{Pt}$)	Maximum Power Density ($mW.cm^{-2}$)
HE00	50	0.753	0.075	691
HE100	55	0.783	0.124	804
HE25	49	0.777	0.116	817
HE50	45	0.747	0.063	953
HE75	65	0.797	0.147	1091

positive shift is observed for Pt/rGO-CB (HE75) hybrid electrocatalyst as compared to that of Pt/CB (44 mV shift) and Pt/rGO (HE100) (14 mV shift) in the half-wave potential. This suggests a noteworthy increase of the ORR activity. Particularly, the half-wave potential for Pt/rGO-CB (HE75) is 0.797 V that is 44 mV higher than Pt/CB and 14 mV higher than Pt/rGO, respectively. Besides, the mass activity of Pt/rGO-CB (HE75) (0.147 mA μg^{-1}) is nearly 2.0 and 1.2 times higher than those of Pt/CB (0.075 mA μg^{-1}) and Pt/rGO (0.124 A mg^{-1}) electrocatalysts (Fig. 6d).

Fig. 7a and 7b represent PEM fuel cell polarization and power output curves of Pt/rGO, Pt/CB and the synthesized hybrid electrocatalysts, at 80 °C and fully humidified conditions. Pt/rGO provides a comparable performance with Pt/CB especially for regions of low and high current density in polarization curve. Comparing both the limiting current densities and the maximum power densities, a significant improvement was achieved by using HE75 among all other hybrid electrocatalysts. Deducing from the cell performance, increasing the graphene amount from 25 to 75 (w:w) in the support material content was remarkably improved power output as a result of better mass transport and more electronically conductive electrode network. That is to say, the current densities achieved at 0.6 V were 0.84, 1.00 and 1.55 A cm^{-2} for Pt/CB (HE00), Pt/rGO (HE100) and Pt/rGO-CB (HE75), respectively. The power output values of all hybrid electrocatalysts were given at Table 2. Additionally, HE50 provides a reasonable performance, especially where mass transport losses dominated the compared to that of CV and LSV results. That can be related to improvement of porosity of obtained GDE network.

The resistance of MEA components is also another important parameter that considerably affect the fuel cell performance. Herein, EIS was utilized for the determination of resistance, both ohmic (R_Ω) and charge transfer (R_{ct}) resistance of the MEAs with different electrocatalysts at cathode. Fig. 7c shows Nyquist plots obtained from *in-situ* EIS analysis of the MEAs with three different electrocatalysts at 0.7 V. The high frequency intercept at Z'_{real} shows the total R_Ω and the diameter of semicircle relates to the R_{ct} which depends on cathode electrocatalyst properties and results from ORR kinetics in cathode. Moreover, reduced diameter of the semicircle indicated the lower impedance of cathode electrocatalyst (the results are summarized in Table 3) [65]. Since the CL fabrication, membrane, GDL, and measurement conditions were the same for all samples, all electrocatalysts had nearly similar R_Ω values (Table 3). The R_{ct} of Pt/rGO-CB

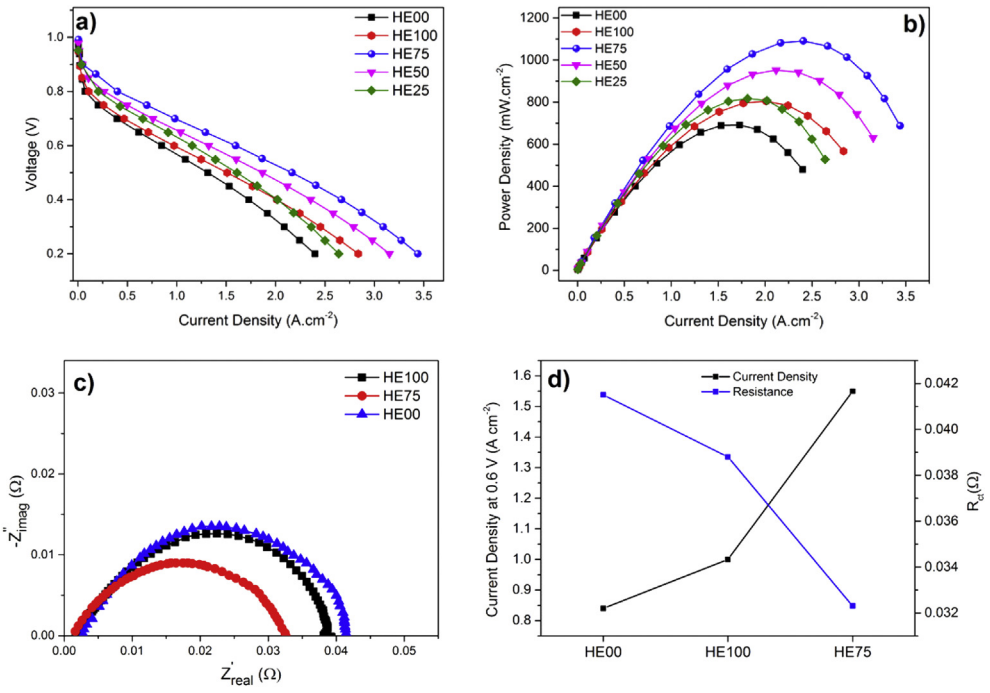

Fig. 7 – H_2/O_2 PEM fuel cell a) Polarization, b) Power output curves for the Pt/rGO-CB electrocatalysts with different composition, c) Electrochemical impedance spectroscopy for Pt/CB, Pt/rGO, and Pt/rGO-CB, and d) Comparison of current density at 0.6 V vs. R_{ct} at 0.7.

Table 3 – Electrochemical properties of MEAs with different electrocatalysts at the cathode.

Samples	$R_{\Omega}(\Omega)$	$R_{ct}(\Omega)$
Pt/CB (**HE00**)	0.0022	0.0415
Pt/rGO (**HE100**)	0.0023	0.0388
Pt/rGO-CB (**HE75**)	0.0017	0.0323

(HE75) was the lower than that of Pt/CB (HE00), Pt/rGO (HE100) electrocatalysts and R_{ct} decreased with increasing current density at 0.6 V. The lower the resistance, the better the fuel cell performance. All these results agreed very well with the PEM fuel cell performance in Fig. 7a and b.

Conclusions

In this study, a facile microwave assisted synthesis of Pt NPs on CB-rGO hybrid support, as electrocatalysts for fuel cell reactions, was performed. Restacking of graphene sheets can be avoided, and impregnation/decoration of Pt NPs on GO-CB hybrid were successfully achieved by mixing of GO and CB at varying ratios. The XRD pattern and XPS analysis of hybrid electrocatalysts proved Pt NPs impregnation on the support. TEM analysis depicted that Pt deposition on rGO and rGO-CB hybrids were homogeneous, and Pt NPs mean diameter was below 2 nm. Conversely, larger Pt NPs and Pt agglomerations were observed when CB was employed as support.

The PEM fuel cell tests clearly shown that the composition of GO-CB hybrid support is very important in terms of electrocatalytic activity and the fuel cell performance of the electrocatalysts since higher amount of CB would block the Pt active sides and lower the catalytic activity. The most promising results on both electrocatalytic activity towards HOR and ORR and fuel cell performance were obtained for the hybrid containing 75% GO (HE75). In accordance with the enhanced fuel cell performance and electrocatalytic activity, electrochemical impedance spectroscopy analysis confirmed better activity of Pt/rGO-CB (HE75) for ORR with lower charge transfer resistance. In conclusion, hybrid structure with low CB content prevented restacking of GO layers, effectively modified the array of graphene and provided more accessible active sites for the reactions.

Acknowledgements

The research leading to these results has received funding from the European Union's Horizon 2020 research and innovation programme under grant agreement No 696656 (Graphene Flagship).

REFERENCES

[1] Marinkas A, Arena F, Mitzel J, Prinz GM, Heinzel A, Peinecke V, et al. Graphene as catalyst support: the influences of carbon additives and catalyst preparation methods on the performance of PEM fuel cells. Carbon 2013;58:139–50.

[2] Şanlı LI, Bayram V, Ghobadi S, Düzen N, Gürsel SA. Engineered catalyst layer design with graphene-carbon black hybrid supports for enhanced platinum utilization in PEM fuel cell. Int J Hydrogen Energy 2017;42:1085–92.

[3] Wan C-H, Zhuang Q-H. Novel layer wise anode structure with improved CO-tolerance capability for PEM fuel cell. Electrochim Acta 2007;52:4111–23.
[4] Gasteiger HA, Kocha SS, Sompalli B, Wagner FT. Activity benchmarks and requirements for Pt, Pt-alloy, and non-Pt oxygen reduction catalysts for PEMFCs. Appl Catal B Environ 2005;56:9–35.
[5] Sui S, Wang X, Zhou X, Su Y, Riffat S, Liu C-j. A comprehensive review of Pt electrocatalysts for the oxygen reduction reaction: nanostructure, activity, mechanism and carbon support in PEM fuel cells. J Mater Chem A 2017;5:1808–25.
[6] Smirnova A, Dong X, Hara H, Vasiliev A, Sammes N. Novel carbon aerogel-supported catalysts for PEM fuel cell application. Int J Hydrogen Energy 2005;30:149–58.
[7] Tour JM. Rice group shows graphene quantum dots beat Pt catalyst. Fuel Cell Bull 2014;2014:13.
[8] Do CL, San Pham T, Nguyen NP, Tran VQ. Properties of Pt/C nanoparticle catalysts synthesized by electroless deposition for proton exchange membrane fuel cell. Adv Nat Sci Nanosci Nanotechnol 2013;4, 035011.
[9] Shao Y, Yin G, Gao Y. Understanding and approaches for the durability issues of Pt-based catalysts for PEM fuel cell. J Power Sources 2007;171:558–66.
[10] Postole G, Auroux A. The poisoning level of Pt/C catalysts used in PEM fuel cells by the hydrogen feed gas impurities: the bonding strength. Int J Hydrogen Energy 2011;36:6817–25.
[11] Li Y, Li Y, Zhu E, McLouth T, Chiu C-Y, Huang X, et al. Stabilization of high-performance oxygen reduction reaction Pt electrocatalyst supported on reduced graphene oxide/carbon black composite. J Am Chem Soc 2012;134:12326–9.
[12] Huang H, Wang X. Recent progress on carbon-based support materials for electrocatalysts of direct methanol fuel cells. J Mater Chem A 2014;2:6266–91.
[13] Su F, Tian Z, Poh CK, Wang Z, Lim SH, Liu Z, et al. Pt nanoparticles supported on nitrogen-doped porous carbon nanospheres as an electrocatalyst for fuel cells. Chem Mater 2009;22:832–9.
[14] Zhang X, Xia G, Huang C, Wang Y. Preparation and characterization of Pt nanoparticles supported on modified graphite nanoplatelet using solution blending method. Int J Hydrogen Energy 2013;38:8909–13.
[15] Sharma S, Ganguly A, Papakonstantinou P, Miao X, Li M, Hutchison JL, et al. Rapid microwave synthesis of CO tolerant reduced graphene oxide-supported platinum electrocatalysts for oxidation of methanol. J Phys Chem C 2010;114:19459–66.
[16] Jha N, Jafri RI, Rajalakshmi N, Ramaprabhu S. Graphene-multi walled carbon nanotube hybrid electrocatalyst support material for direct methanol fuel cell. Int J Hydrogen Energy 2011;36:7284–90.
[17] Barbir F. PEM fuel cells. Fuel Cell Technology. Springer; 2006. p. 27–51.
[18] Wu J, Yuan XZ, Martin JJ, Wang H, Zhang J, Shen J, et al. A review of PEM fuel cell durability: degradation mechanisms and mitigation strategies. J Power Sources 2008;184:104–19.
[19] Schmittinger W, Vahidi A. A review of the main parameters influencing long-term performance and durability of PEM fuel cells. J Power Sources 2008;180:1–14.
[20] Tamaki T, Wang H, Oka N, Honma I, Yoon S-H, Yamaguchi T. Correlation between the carbon structures and their tolerance to carbon corrosion as catalyst supports for polymer electrolyte fuel cells. Int J Hydrogen Energy 2018;43:6406–12.
[21] Wong WY, Daud WRW, Mohamad AB, Loh KS. Effect of temperature on the oxygen reduction reaction kinetic at nitrogen-doped carbon nanotubes for fuel cell cathode. Int J Hydrogen Energy 2015;40:11444–50.
[22] Calvillo L, Gangeri M, Perathoner S, Centi G, Moliner R, Lázaro MJ. Synthesis and performance of platinum supported on ordered mesoporous carbons as catalyst for PEM fuel cells: effect of the surface chemistry of the support. Int J Hydrogen Energy 2011;36:9805–14.
[23] Sebastián D, Calderón JC, González-Expósito JA, Pastor E, Martínez-Huerta MV, Suelves I, et al. Influence of carbon nanofiber properties as electrocatalyst support on the electrochemical performance for PEM fuel cells. Int J Hydrogen Energy 2010;35:9934–42.
[24] Dicks AL. The role of carbon in fuel cells. J Power Sources 2006;156:128–41.
[25] Şanlı LI, Yarar B, Bayram V, Gürsel SA. Electrosprayed catalyst layers based on graphene–carbon black hybrids for the next-generation fuel cell electrodes. J Mater Sci 2017;52:2091–102.
[26] Sevim Yılmaz M, Kaplan BY, Metin Ö, Gürsel SA. A facile synthesis and assembly of ultrasmall Pt nanoparticles on reduced graphene oxide-carbon black hybrid for enhanced performance in PEMFC. Mater Des 2018;151:29–36.
[27] Daş E, Yurtcan AB. Effect of carbon ratio in the polypyrrole/carbon composite catalyst support on PEM fuel cell performance. Int J Hydrogen Energy 2016;41:13171–9.
[28] Navaei Alvar E, Zhou B, Eichhorn SH. Composite-supported Pt catalyst and electrosprayed cathode catalyst layer for polymer electrolyte membrane fuel cell. Int J Energy Res 2017;41:1626–41.
[29] Kim T, Xie T, Jung WS, Popov BN. Development of ultra–low highly active and durable hybrid compressive platinum lattice cathode catalysts for polymer electrolyte membrane fuel cells. Int J Hydrogen Energy 2017;42:12507–20.
[30] Geim AK, Novoselov KS. The rise of graphene. Nat Mater 2007;6:183–91.
[31] Quesnel E, Roux F, Emieux F, Faucherand P, Kymakis E, Volonakis G, et al. Graphene-based technologies for energy applications, challenges and perspectives. 2D Mater 2015;2, 030204.
[32] Daş E, Gürsel SA, Şanli LI, Yurtcan AB. Comparison of two different catalyst preparation methods for graphene nanoplatelets supported platinum catalysts. Int J Hydrogen Energy 2016;41:9755–61.
[33] Daş E, Alkan Gürsel S, Işıkel Şanlı L, Bayrakçeken Yurtcan A. Thermodynamically controlled Pt deposition over graphene nanoplatelets: effect of Pt loading on PEM fuel cell performance. Int J Hydrogen Energy 2017;42:19246–56.
[34] Yazici MS, Azder MA, Salihoglu O, Boyaci San FG. Ultralow Pt loading on CVD graphene for acid electrolytes and PEM fuel cells. Int J Hydrogen Energy 2018;43(40):18572–7. https://doi.org/10.1016/j.ijhydene.2018.06.020.
[35] Soo LT, Loh KS, Mohamad AB, Daud WRW, Wong WY. An overview of the electrochemical performance of modified graphene used as an electrocatalyst and as a catalyst support in fuel cells. Appl Catal A 2015;497:198–210.
[36] Cho SH, Yang HN, Lee DC, Park SH, Kim WJ. Electrochemical properties of Pt/graphene intercalated by carbon black and its application in polymer electrolyte membrane fuel cell. J Power Sources 2013;225:200–6.
[37] Jafri RI, Rajalakshmi N, Dhathathreyan KS, Ramaprabhu S. Nitrogen doped graphene prepared by hydrothermal and thermal solid state methods as catalyst supports for fuel cell. Int J Hydrogen Energy 2015;40:4337–48.
[38] Lee D, Hwang S. Effect of loading and distributions of Nafion ionomer in the catalyst layer for PEMFCs. Int J Hydrogen Energy 2008;33:2790–4.
[39] Park S, Shao Y, Wan H, Rieke PC, Viswanathan VV, Towne SA, et al. Design of graphene sheets-supported Pt catalyst layer in PEM fuel cells. Electrochem Commun 2011;13:258–61.

[40] Lee WH, Yang HN, Park KW, Choi BS, Yi SC, Kim WJ. Synergistic effect of boron/nitrogen co-doping into graphene and intercalation of carbon black for Pt-BCN-Gr/CB hybrid catalyst on cell performance of polymer electrolyte membrane fuel cell. Energy 2016;96:314–24.
[41] Pham K-C, McPhail DS, Mattevi C, Wee AT, Chua DH. Graphene-carbon nanotube hybrids as robust catalyst supports in proton exchange membrane fuel cells. J Electrochem Soc 2016;163:F255–63.
[42] Vinayan B, Ramaprabhu S. Platinum–TM (TM= Fe, Co) alloy nanoparticles dispersed nitrogen doped (reduced graphene oxide-multiwalled carbon nanotube) hybrid structure cathode electrocatalysts for high performance PEMFC applications. Nanoscale 2013;5:5109–18.
[43] Fu K, Wang Y, Mao L, Jin J, Yang S, Li G. Facile one-pot synthesis of graphene-porous carbon nanofibers hybrid support for Pt nanoparticles with high activity towards oxygen reduction. Electrochim Acta 2016;215:427–34.
[44] Abdolhosseinzadeh S, Sadighikia S, Alkan Gürsel S. Scalable synthesis of sub-nanosized platinum-reduced graphene oxide composite by an ultraprecise photocatalytic method. ACS Sustain Chem Eng 2018;6:3773–82.
[45] Pinchuk OA, Dundar F, Ata A, Wynne KJ. Improved thermal stability, properties, and electrocatalytic activity of sol-gel silica modified carbon supported Pt catalysts. Int J Hydrogen Energy 2012;37:2111–20.
[46] Seger B, Kamat PV. Electrocatalytically active graphene-platinum nanocomposites. Role of 2-D carbon support in PEM fuel cells. J Phys Chem C 2009;113:7990–5.
[47] Zhang J, Yang H, Shen G, Cheng P, Zhang J, Guo S. Reduction of graphene oxide via L-ascorbic acid. Chem Commun 2010;46:1112–4.
[48] Ghosh A, Basu S, Verma A. Graphene and functionalized graphene supported platinum catalyst for PEMFC. Fuel Cells 2013;13:355–63.
[49] Şanlı LI, Bayram V, Yarar B, Ghobadi S, Gürsel SA. Development of graphene supported platinum nanoparticles for polymer electrolyte membrane fuel cells: effect of support type and impregnation–reduction methods. Int J Hydrogen Energy 2016;41:3414–27.
[50] Hsieh SH, Hsu MC, Liu WL, Chen WJ. Study of Pt catalyst on graphene and its application to fuel cell. Appl Surf Sci 2013;277:223–30.
[51] Galema SA. Microwave chemistry. Chem Soc Rev 1997;26:233–8.
[52] Hsieh C-T, Hung W-M, Chen W-Y, Lin J-Y. Microwave-assisted polyol synthesis of Pt–Zn electrocatalysts on carbon nanotube electrodes for methanol oxidation. Int J Hydrogen Energy 2011;36:2765–72.
[53] Yang HN, Lee DC, Park KW, Kim WJ. Platinum–boron doped graphene intercalated by carbon black for cathode catalyst in proton exchange membrane fuel cell. Energy 2015;89:500–10.
[54] Li Y, Gao W, Ci L, Wang C, Ajayan PM. Catalytic performance of Pt nanoparticles on reduced graphene oxide for methanol electro-oxidation. Carbon 2010;48:1124–30.
[55] Si Y, Samulski ET. Exfoliated graphene separated by platinum nanoparticles. Chem Mater 2008;20:6792–7.
[56] Jung JH, Park HJ, Kim J, Hur SH. Highly durable Pt/graphene oxide and Pt/C hybrid catalyst for polymer electrolyte membrane fuel cell. J Power Sources 2014;248:1156–62.
[57] Liu X, Li L, Meng C, Han Y. Palladium nanoparticles/defective graphene composites as oxygen reduction electrocatalysts: a first-principles study. J Phys Chem C 2012;116:2710–9.
[58] Guo H-L, Wang X-F, Qian Q-Y, Wang F-B, Xia X-H. A green approach to the synthesis of graphene nanosheets. ACS Nano 2009;3:2653–9.
[59] Chiang Y-C, Liang C-C, Chung C-P. Characterization of platinum nanoparticles deposited on functionalized graphene sheets. Materials 2015;8:6484–97.
[60] Mondal A, Jana NR. Surfactant-free, stable noble metal–graphene nanocomposite as high performance electrocatalyst. ACS Catal 2014;4:593–9.
[61] Roth C, Goetz M, Fuess H. Synthesis and characterization of carbon-supported Pt–Ru–WOx catalysts by spectroscopic and diffraction methods. J Appl Electrochem 2001;31:793–8.
[62] Simonov P, Romanenko A, Prosvirin I, Kryukova G, Chuvilin A, Bogdanov S, et al. Electrochemical behaviour of quasi-graphitic carbons at formation of supported noble metal catalysts. Stud Surf Sci Catal 1998;118:15–30.
[63] Qiu J-D, Wang G-C, Liang R-P, Xia X-H, Yu H-W. Controllable deposition of platinum nanoparticles on graphene as an electrocatalyst for direct methanol fuel cells. T J Phys Chem C 2011;115:15639–45.
[64] Cho S, Yang H, Lee D, Park S, Kim W. Electrochemical properties of Pt/graphene intercalated by carbon black and its application in polymer electrolyte membrane fuel cell. J Power Sources 2013;225:200–6.
[65] Yuan X, Wang H, Sun JC, Zhang J. AC impedance technique in PEM fuel cell diagnosis—a review. Int J Hydrogen Energy 2007;32:4365–80.